Comparison of classical and quantum spectra for a totally bound potential

1981 J. Phys. A: Math. Gen. 14 L477

(http://iopscience.iop.org/0305-4470/14/12/001)

J. Phys. A: Math. Gen. **14** (1981) L477–L484. Printed in Great Britain

LETTER TO THE EDITOR

Comparison of classical and quantal spectra for a totally bound potential

R A Pullen and A R Edmonds

Blackett Laboratory, Imperial College, London SW7 2AZ, England

Received 8 September 1981

Abstract. The quantal energy spectrum is compared with the classical motion for the totally bound potential $\frac{1}{2}(x^2+y^2)+\alpha x^2y^2$. The classical phase space is filled with regular trajectories at lower energies, but as the energy is increased both regular and irregular trajectories are observed to coexist. At very high energies the classical phase space is almost totally filled with irregular trajectories. The work reported in this Letter is similar to that performed by the authors on the Hénon–Heiles potential with the purpose of testing the prediction by Percival that there is good agreement between the amount of classical irregular motion and the proportion of energy eigenvalues sensitive to small changes in the perturbation parameter. However, the potential investigated in this Letter has several computational advantages over the Hénon–Heiles potential as well as avoiding complications due to quantum mechanical tunnelling. The results show good agreement with Percival's predictions.

1. Introduction

Percival (1973) has predicted that, in the semiclassical limit, the quantal energy spectrum of a dynamical system consists of a regular and an irregular part. In the general case for an inseparable Hamiltonian of N degrees of freedom the regular quantal spectrum corresponds, in the limit $\hbar \to 0$, to regular classical motion, where trajectories lie on N-dimensional invariant toroids. The irregular quantal spectrum corresponds to irregular trajectories which are associated with unstable orbits (Contopoulos 1971) which do not lie on invariant toroids. Energy eigenvalues of the irregular spectrum are more sensitive to a slowly changing or fixed perturbation than those of the regular spectrum. At low energies the classical phase space is dominated by regular trajectories, but as the energy increases a greater volume of phase space is taken up by irregular trajectories.

Pomphrey (1974), Noid *et al* (1980), Weissman and Jortner (1981) and Pullen and Edmonds (1981) have made numerical studies of a modified Hénon–Heiles Hamiltonian (Hénon and Heiles 1964)

$$H=\tfrac{1}{2}(p_x^2+p_y^2+x^2+y^2)+\alpha(x^2y-\tfrac{1}{3}y^3) \tag{1.1}$$

where $p_x=\dot{x}$, $p_y=\dot{y}$ $(m=1)$, comparing the quantal spectrum to the classical motion. Pomphrey (1974) and Pullen and Edmonds (1981) found that for $\alpha=0.088$ there were a number of eigenvalues at higher energies which had large second differences, Δ_i^2, with respect to small variations in the perturbation parameter, α. Δ_i^2 is given by

$$\Delta_i^2=|[E_i(\alpha+\Delta\alpha)-E_i(\alpha)]-[E_i(\alpha)-E_i(\alpha-\Delta\alpha)]|. \tag{1.2}$$

0305-4470/81/120477+08$01.50

These eigenvalues belong to the irregular quantal spectrum and occur above a critical energy, E_c, which is the energy at which the classical motion begins its transition from being dominated by regular motion to being dominated by irregular motion. Pullen and Edmonds (1981) showed that these large second differences correspond to avoided crossings. Noid *et al* (1980) and Weissman and Jortner (1981) made similar investigations with $\alpha = 0.1118$ and $\alpha = 0.085$ respectively. Their results appear to conflict with those of Pomphrey (1974) and Pullen and Edmonds (1981).

In this Letter we have investigated the potential

$$U = \tfrac{1}{2}(x^2 + y^2) + \alpha x^2 y^2 \tag{1.3}$$

because it has a number of advantages over the Hénon–Heiles potential. Firstly, the Hénon–Heiles potential has no strictly bound quantum mechanical states due to tunnelling, though for small excitations the error in assuming discrete eigenvalues is small. This causes problems when evaluating the eigenvalues by diagonalising the truncated matrix $\tilde{H}$ defined by $\tilde{H}_{ij} = \langle \psi_i | \hat{H} | \psi_j \rangle$, where ψ_i and ψ_j are basis functions which are linear combinations of the eigenfunctions of the unperturbed harmonic oscillator. It is necessary to make the Hénon–Heiles matrix sufficiently large so that the computed eigenvalues will converge to the required precision. However, if the matrix is made too large, the higher eigenvalues will begin to diverge due to the influence of basis functions with a significant proportion of their probability densities outside the 'bounding triangle' of the Hénon–Heiles potential. This causes accuracy problems and limits the range of energy available for investigation. The potential (1.3) has only discrete quantum mechanical states, and so increasing the order of the matrix allows us to obtain the required accuracy for all the eigenvalues under investigation. Also there are more eigenvalues available for investigation, and the symmetry of the potential allows us to split our Hamiltonian matrix into submatrices reducing the computer storage required. At those energies under study $\hbar$ has an effectively smaller value than in previous investigations with the Hénon–Heiles potential, and so we might expect a closer correspondence between classical and quantal spectra as we are nearer the semiclassical limit.

2. Computation of classical orbits

The classical equations of motion obtained from the Hamiltonian (1.1) are

$$\ddot{x} = -x - 2\alpha x y^2 \qquad \ddot{y} = -y - 2\alpha y x^2. \tag{2.1}$$

We used the fifth-order Runge–Kutta–Nyström method (Henrici 1962, p 173) to compute the classical trajectories. Tests were made on the accuracy of the computed trajectories by continually checking that the variation in energy was small, and by recomputation with a different step length.

Figure 1 illustrates a contour plot for the potential (1.3) which has the symmetry of the C_{4v} point group.

Surface of section pictures (Poincaré 1897) have been produced (figures 2(*a*)–2(*c*) illustrate a few of these) for a variety of energies, showing the transition from almost totally regular motion at low energies to almost totally irregular motion at high energies. Conservation of energy restricts any trajectory in four-dimensional phase space to a three-dimensional energy shell. At a particular energy, therefore, the restriction $x = 0$ defines a two-dimensional surface in phase space. Each time a

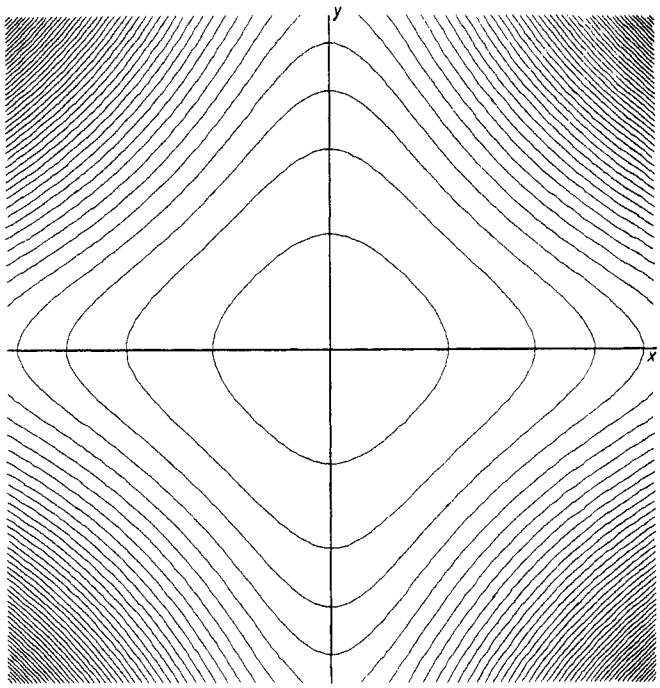

Figure 1. Contour plot for the potential (1.3) with $\alpha = 0.05$. Both axes range from -10 to $+10$.

particular trajectory passes through the surface, i.e. each time it crosses the y axis, a point is plotted at the position of intersection (y, p_y). We employ a first-order interpolation process to reduce inaccuracies introduced by using a finite step length.

Regular regions on the surface of section plots are characterised by sets of invariant curves, whereas irregular regions are characterised by a random-like distribution of intersection points. For our choice of perturbation parameter ($\alpha = 0.05$), the surface of section pictures show that the motion is almost wholly regular below $E = 15$ (see figure 2(a)). However, as we increase the energy above this value, some of the invariant curves begin to break up (see figures 2(b) and 2(c)), and at energies above $E = 50$ the motion appears to be almost wholly irregular.

We are not concerned in this Letter with the finer details of the surface of section pictures, but we are simply using them to illustrate the smooth transition from a phase space occupied almost wholly by regular trajectories to one occupied almost wholly by irregular trajectories.

3. Computation of quantal energy spectrum

We consider the quantum mechanical Hamiltonian in cartesian coordinates

$$\hat{H} = -\frac{1}{2}\frac{\partial^2}{\partial x^2} - \frac{1}{2}\frac{\partial^2}{\partial y^2} + \tfrac{1}{2}(x^2 + y^2) + \alpha x^2 y^2 \tag{3.1}$$

where $\hbar$ has been put equal to 1. Eigenvalues of this Hamiltonian were calculated by

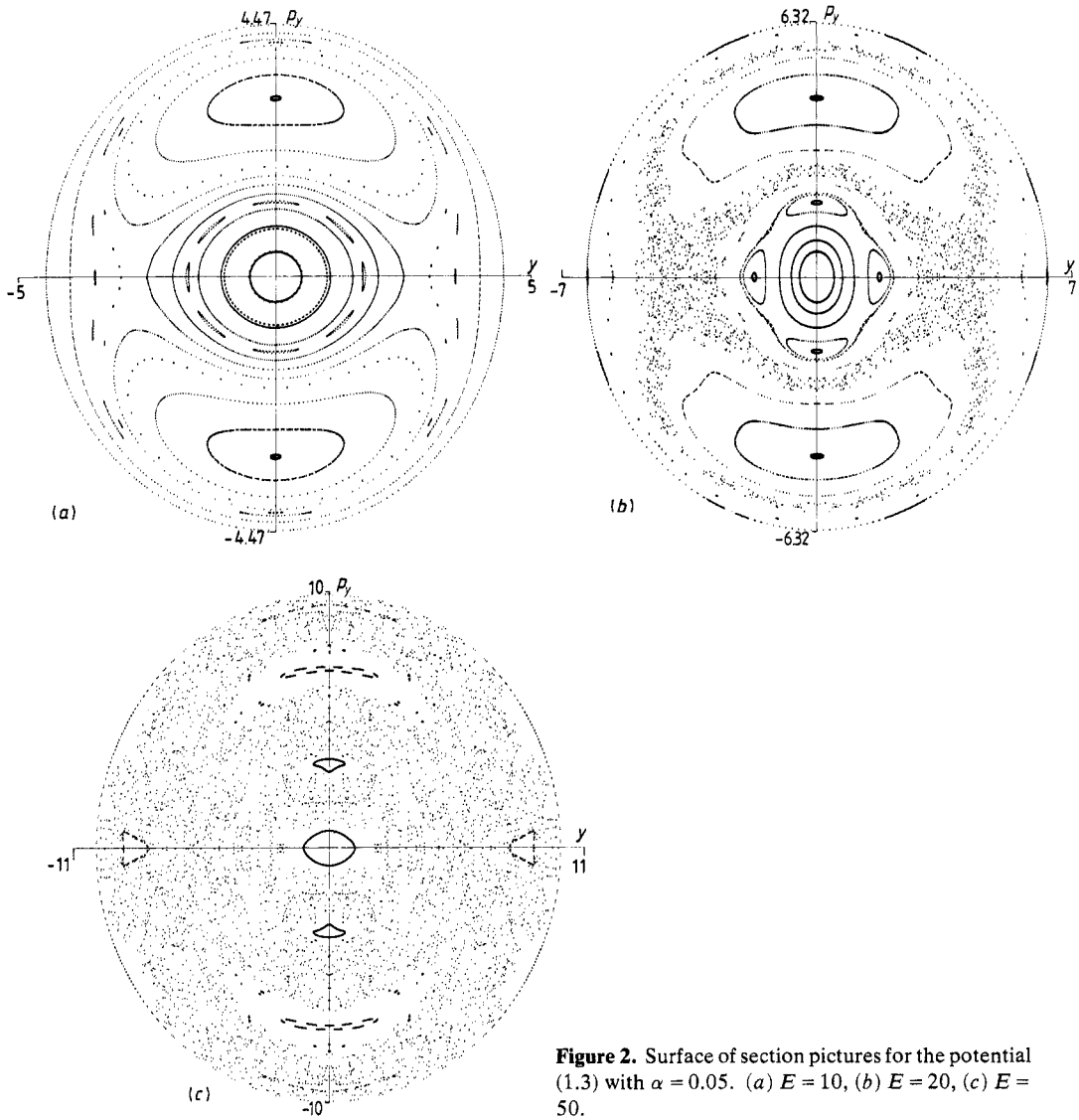

Figure 2. Surface of section pictures for the potential (1.3) with $\alpha = 0.05$. (*a*) $E = 10$, (*b*) $E = 20$, (*c*) $E = 50$.

diagonalising the matrix $\tilde{H}$ defined by $\tilde{H}_{ij} = \langle \psi_i | \hat{H} | \psi_j \rangle$ where ψ_i and ψ_j are basis functions which are linear combinations of the eigenfunctions of the unperturbed harmonic oscillator with potential

$$U = \tfrac{1}{2}(x^2 + y^2). \tag{3.2}$$

The normalised eigenfunctions for the potential (3.2) are

$$\psi_{n_x n_y}(x, y) = \frac{1}{(\pi 2^{n_x+n_y} n_x! n_y!)^{1/2}} H_{n_x}(x) \exp(-x^2/2) H_{n_y}(y) \exp(-y^2/2) \tag{3.3}$$

where H_{n_x} and H_{n_y} are Hermite polynomials.

It is important to take account of the full symmetry of the Hamiltonian for two reasons. Firstly we can divide the matrix $\tilde{H}$ into submatrices and so reduce computational time and storage, and secondly we can be sure that large second differences calculated by equation (1.2) are due to avoided crossings and not crossings.

The full symmetry group of the Hamiltonian (3.1) is the C_{4v} point group. There are eight elements of this group: E, C_2, C_4, C_4^3, σ_1, σ_2, σ_1', σ_2'. E is the unit element, and C_2, C_4 and C_4^3 are rotations by 180°, 90° and 270° respectively. σ_1' and σ_2' are reflections about the x and y axes and σ_1 and σ_2 are reflections about these same axes rotated by 45°. Table 1 is the character table for the irreducible representations of C_{4v}. A_1, A_2, B_1, B_2 and E label the different irreducible representations. We can see immediately from the presence of an irreducible representation of dimension two that the perturbation does not completely break the degeneracy of the unperturbed system. We now have eigenstates which are non-degenerate and have A_1, A_2, B_1 or B_2 symmetry, or we have doubly degenerate states with E symmetry.

Table 1. Character table of the irreducible representations of the C_{4v} point group.

	E	C_2	$2C_4$	2σ	$2\sigma'$
A_1	1	1	1	1	1
A_2	1	1	1	−1	−1
B_1	1	1	−1	1	−1
B_2	1	1	−1	−1	1
E	2	−2	0	0	0

The basis functions we have chosen are linear combinations of the eigenfunctions of the unperturbed harmonic oscillator and transform according to the irreducible representations of C_{4v}:

$$N \exp[-(x^2+y^2)/2](H^{e}_{n_1}(x)H^{e}_{n_2}(y)+H^{e}_{n_1}(y)H^{e}_{n_2}(x)), \tag{3.4}$$

$$N \exp[-(x^2+y^2)/2](H^{o}_{n_1}(x)H^{o}_{n_2}(y)-H^{o}_{n_1}(y)H^{o}_{n_2}(x)), \tag{3.5}$$

$$N \exp[-(x^2+y^2)/2](H^{e}_{n_1}(x)H^{e}_{n_2}(y)-H^{e}_{n_1}(y)H^{e}_{n_2}(x)), \tag{3.6}$$

$$N \exp[-(x^2+y^2)/2](H^{o}_{n_1}(x)H^{o}_{n_2}(y)+H^{o}_{n_1}(y)H^{o}_{n_2}(x)), \tag{3.7}$$

where $H^{e}_{n}(x)$ and $H^{e}_{n}(y)$ are Hermite polynomials with even integer values of n and $H^{o}_{n}(x)$ and $H^{o}_{n}(y)$ are Hermite polynomials with odd integer values of n. N is a normalisation constant. Basis functions defined by (3.4), (3.5), (3.6) and (3.7) transform according to the irreducible representations A_1, A_2, B_1 and B_2 respectively.

We have confined our investigation to non-degenerate eigenvalues as the order of the E symmetry submatrix (whose basis functions are made up of combinations of even and odd integer Hermite polynomials) requires too much computer storage space for accurate evaluation of the higher E symmetry eigenvalues.

Values of non-zero matrix elements may be calculated using the orthogonality relation

$$\frac{1}{(2^{n+n'}n!n'!\pi)^{1/2}}\int_{-\infty}^{\infty}\exp(-q^2)H_n(q)H_{n'}(q)\,dq=\delta_{nn'} \tag{3.8}$$

together with the recursion relation

$$qH_n(q) = nH_{n-1}(q) + \tfrac{1}{2}H_{n+1}(q) \tag{3.9}$$

to obtain

$$\begin{aligned}\text{Matrix element} = {} & \tfrac{1}{4}\alpha[\{(n_1n_1')^{1/2} + [(n_1+1)(n_1'+1)]^{1/2}\}\delta_{n_1n_1'} + [(n_1+1)n_1']^{1/2}\delta_{n_1n_1'-2} \\ & + [n_1(n_1'+1)]^{1/2}\delta_{n_1n_1'+2}] \times [\{(n_2n_2')^{1/2} + [(n_2+1)(n_2'+1)]^{1/2}\}\delta_{n_2n_2'} \\ & + [(n_2+1)n_2']^{1/2}\delta_{n_2n_2'-2} + [n_2(n_2'+1)]^{1/2}\delta_{n_2n_2'+2}] \\ & \pm \tfrac{1}{4}\alpha[\{(n_1n_2')^{1/2} + [(n_1+1)(n_2'+1)]^{1/2}\}\delta_{n_1n_2'} + [(n_1+1)n_2']^{1/2}\delta_{n_1n_2'-2} \\ & + [n_1(n_2'+1)]^{1/2}\delta_{n_1n_2'+2}] \times [\{(n_2n_1')^{1/2} + [(n_2+1)(n_1'+1)]^{1/2}\}\delta_{n_2n_1'} \\ & + [(n_2+1)n_1']^{1/2}\delta_{n_2n_1'-2} + [n_2(n_1'+1)]^{1/2}\delta_{n_2n_1'+2}]\end{aligned} \tag{3.10}$$

where the positive sign is taken by basis functions of the type (3.4) and (3.7) and the negative sign is taken by basis functions of the type (3.5) and (3.6).

Truncated matrices were diagonalised using Householder reduction to tridiagonal form (see Wilkinson and Reinsch 1971, pp 212–6) followed by the method of bisection (see Wilkinson and Reinsch 1971, pp 249–56). It was necessary to make the truncated matrices sufficiently large so that the computed eigenvalues would converge to the required precision (an accuracy of four decimal places was obtained for the higher eigenvalues by diagonalising matrices of order 300). We have considered eigenvalues computed up to $E = 50$.

4. Results and conclusions

The purpose of this Letter has been to test further the prediction of Percival (1973) that in the semiclassical limit irregular classical motion corresponds to an irregular quantal spectrum. As discussed in the Introduction, similar investigations to those made in this Letter have been made on the Hénon–Heiles potential, but the new potential has the advantage that we are dealing with a totally bound system nearer the semiclassical limit.

We have identified eigenvalues as being irregular if they have large second differences corresponding to avoided crossings. Table 2 summarises our results. We

Table 2. Number of eigenvalues with low, intermediate and high second differences in a given energy range.

Energy range	Low	Intermediate	High	Energy range	Low	Intermediate	High
11–13	6	5	0	31–33	3	11	9
13–15	6	5	0	33–35	0	14	10
15–17	5	8	0	35–37	1	8	16
17–19	5	10	0	37–39	0	6	21
19–21	1	11	3	39–41	0	6	19
21–23	3	9	4	41–43	1	5	22
23–25	2	9	6	43–45	0	7	24
25–27	2	17	2	45–47	0	2	26
27–29	2	8	11	47–49	0	5	28
29–31	2	11	5	49–51	0	3	30

have used equation (1.2) to compute the second differences for $\Delta\alpha = 0.00125$, and have sorted the eigenvalues into three categories, low, intermediate and high second differences.

As we have taken symmetry into account we would expect all our large second differences to correspond to avoided crossings. This follows from a theorem of von Neumann and Wigner (1929), Teller (1937) and Arnol'd (1978) which forbids crossings between energy levels of the same symmetry for a one-parameter generic real Hamiltonian system. We have checked this numerically for all large second differences obtained and found this to be the case (figure 3 illustrates a sample of avoided crossings).

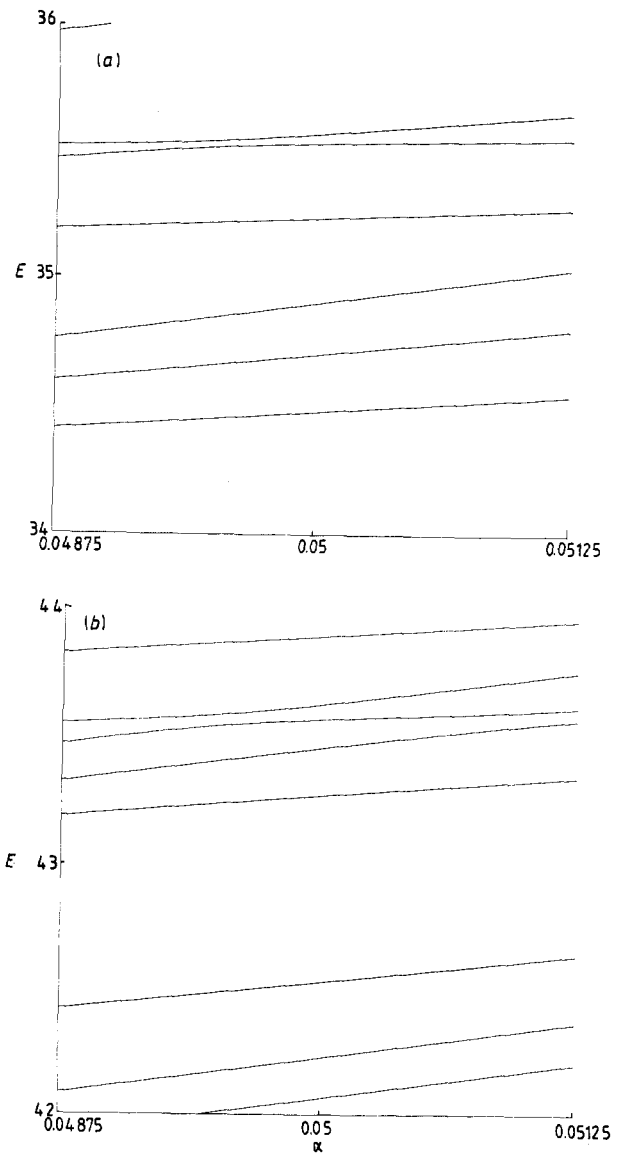

Figure 3. Energy versus perturbation parameter plots for eigenvalues of A_1 symmetry.

The results of table 2 (which are also illustrated by figure 4) indicate a gradual transition from regular quantal behaviour at low energies ($E \approx 20$) to irregular quantal behaviour at high energies (above $E \approx 50$). This corresponds well with the classical transition from regularity to irregularity over the same region of energy.

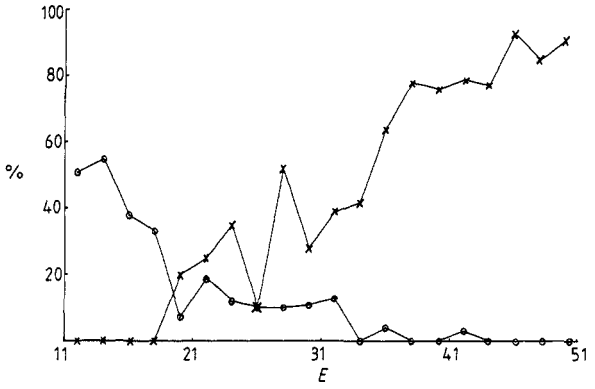

Figure 4. Graph illustrating the percentage of non-degenerate eigenvalues with low second differences (circles) and high second differences (crosses). Each circle or cross represents the percentage calculated over a range of energy $\Delta E = 2$. Intermediate percentages are not plotted.

Acknowledgment

One of us (RP) would like to thank the Science Research Council for a postgraduate grant.

References

Arnol'd V I 1978 *Mathematical Methods of Classical Mechanics* (New York: Springer) appendix 10
Contopoulos G 1971 *Astron. J.* **76** 147–56
Hénon M and Heiles C 1964 *Astron. J.* **69** 73–9
Henrici P 1962 *Discrete Variable Methods in Ordinary Differential Equations* (New York: Wiley)
von Neumann J and Wigner E P 1929 *Z. Phys.* **30** 467–70
Noid D W, Koszykowski M L, Tabor M and Marcus R A 1980 *J. Chem. Phys.* **72** 6169–75
Percival I C 1973 *J. Phys. B: At. Mol. Phys.* **6** L229–32
Poincaré H 1897 *New Methods of Celestial Mechanics* vol 3, ch 27 (Transl. NASA Washington DC 1967)
Pomphrey N 1974 *J. Phys. B: At. Mol. Phys.* **7** 1909–15
Pullen R A and Edmonds A R 1981 *J. Phys. A: Math. Gen.* **14** L319–27
Teller E 1937 *J. Phys. Chem.* **41** 109–16
Weissman Y and Jortner J 1981 *Chem. Phys. Lett.* **78** 224–9
Wilkinson J H and Reinsch C 1971 *Handbook for Automatic Computation* (Berlin: Springer)